

Monte Carlo simulations of the $L1_0$ long-range order relaxation in dimensionally reduced systems

This article has been downloaded from IOPscience. Please scroll down to see the full text article.

2007 J. Phys.: Condens. Matter 19 036218

(<http://iopscience.iop.org/0953-8984/19/3/036218>)

View [the table of contents for this issue](#), or go to the [journal homepage](#) for more

Download details:

IP Address: 129.252.86.83

The article was downloaded on 28/05/2010 at 15:23

Please note that [terms and conditions apply](#).

Monte Carlo simulations of the $L1_0$ long-range order relaxation in dimensionally reduced systems

Mohammed Allalen¹, Tarik Mehaddene^{2,4} and Hamid Bouzar³

¹ Universität Osnabrück, Fachbereich Physik, D-49069 Osnabrück, Germany

² Physik-Department E13, Technische Universität München, 85747 Garching, Germany

³ LPCQ, University Mouloud Mammeri, 15000 Tizi-Ouzou, Algeria

E-mail: mallalen@uos.de and mtarik@ph.tum.de

Received 14 August 2006, in final form 29 November 2006

Published 5 January 2007

Online at stacks.iop.org/JPhysCM/19/036218

Abstract

Monte Carlo simulations have been performed to investigate the relaxation of the $L1_0$ long-range order in dimensionally reduced systems. The effect of the number of (001)-type monoatomic layers and of the pair interaction energies on these kinetics has been examined. The vacancy migration energies have been deduced from the Arrhenius plots of the relaxation times. A substantial increase in the migration energy for small film thickness is observed. The results agree with previous Monte Carlo simulations and with recent experimental results in $L1_0$ thin films and multilayers.

1. Introduction

Binary ferromagnetic materials with the $L1_0$ structure are promising candidates for use as magneto-optical recording media thanks to their high magnetic anisotropy. The $L1_0$ structure (also called the CuAu structure) is based on the face centred lattice of tetragonal symmetry. It is built by alternating {001} pure planes of each type of atom. Three variants are present in the $L1_0$ structure: x -, y - and z -variants. The z -variant is built when the (001) pure atomic planes are stacked along the [001] direction, whereas the x - and y -variants are obtained when the pure atomic planes are stacked along the [100] and [010] directions, respectively. Among the most investigated systems are Co–Pt, Fe–Pt and Fe–Pd. They present a tetragonal distortion of the lattice ($c/a < 1$) [1–3] and exhibit a uniaxial magnetocrystalline anisotropy in the range $K_1 = 1\text{--}10 \text{ MJ m}^{-3}$ with the c -axis as the easy magnetization axis. The discovery of the interesting properties of these materials dates back to the 1930s. They have been, however, the topic of many intensive experimental and theoretical works in the last decades (see [4, 5] and references therein). A good knowledge of the ordering process and of its dynamics is a necessary step in any extensive research into these systems.

⁴ Author to whom any correspondence should be addressed.

A systematic study of the physical, thermodynamic and kinetic properties of the Fe–Pd, Fe–Pt and Co–Pt ordered alloys is now in progress. Atomic migration has been investigated using experimental resistivity measurements and lattice dynamics to deduce the atomic migration energies at different temperatures and states of atomic order. The study is almost complete in FePd [6–8, 10], whereas the other two systems are still under investigation. In parallel to these experimental investigations, numerical simulations of the thermodynamic properties and structural kinetics have been performed using Monte Carlo methods and molecular dynamics [5, 9]. L1₀-ordering kinetics in FePt nanolayers have been recently simulated using a Monte Carlo method based on pair interaction energies deduced from the cluster expansion method [11]. The results indicate a clear stabilization effect of the Pt surface on the *z*-variant of the L1₀ structure.

In this paper we present systematic Monte Carlo simulations of the L1₀ long-range order relaxation in dimensionally reduced systems. For this purpose the isothermal relaxation of the long-range order (LRO) parameter is investigated in the *z*-variant of the L1₀ structure, with different numbers of (001)-type monatomic layers. We first present the effect of the film thickness on the order–disorder transition for different ordering energies. To get more insight into the order–order kinetics, the isothermal relaxation of a short-range order parameter, namely the antisite pair correlation (APC) parameter, is simulated along with the LRO parameter. Finally, the Arrhenius plots of the relaxation times are used to deduce the vacancy migration energy for different film thicknesses. The present work attempts to find out to what extent the kinetics in dimensionally reduced L1₀ compounds are influenced in comparison with processes taking place in bulk systems.

2. Simulation method

Stochastic techniques based on random processes, such as Monte Carlo methods, have been used to solve a wide variety of problems [12]. They have been established as a powerful technique for investigating the kinetics of the relaxation of the long-range order in intermetallics [13–15].

Dimensionally reduced L1₀ systems have been modelled by a set of N_A atoms A and N_B atoms B distributed on a perfect face-centred-cubic rigid lattice with a linear size $L = 64$ along the [100] and [010] directions and variable thickness M along the [001] direction. To conform to the stoichiometry of the L1₀ structure, there are as many A atoms as B atoms. Periodic boundary conditions have been used along the *x*- and *y*-axes whereas these have been removed along the *z*-axis. As a result of symmetry breaking, relaxation and reconstruction processes often take place at the free surfaces of real thin films inducing local defects and building extra units or clusters. As surface-induced defects are beyond the scope of the present study, we restrict ourselves to flat and ideal surfaces. Assuming interactions up to next nearest-neighbours only, the total energy of the system can be expressed in a general AB_v model by an Ising Hamiltonian [16]

$$\mathcal{H} = \frac{1}{2} \sum_{i,j} V_{ij} \sigma_i \sigma_j \quad (1)$$

where the sum extends over all the nearest and the next nearest-neighbour pairs and i and j are generic indices sweeping all the lattice. The occupation operator on site i , σ_i , can take the values: +1, –1 and 0 if site i is occupied by an A atom, a B atom or a vacancy *v*, respectively. V_{ij} are the pair interaction energies between atoms at sites i and j . For convenience the pair interactions can be labelled by the shell index n , which in the present work can take the value 1 and 2 for the nearest-neighbours and the next nearest-neighbours, respectively. Following

earlier works in bulk L1₀ compounds [17], phenomenological pair interaction energies are used with a constant value of the first pair interaction $V_1 = 20$ meV and different values of the second pair interaction V_2 . We have chosen to restrict our study to symmetric interaction energies and neglect the vacancy–atom interactions:

$$V_{vA} = V_{vB} = 0; \quad V_{AA} = V_{BB} = -V_{AB}. \quad (2)$$

Vacancy–atom interactions are usually considered to take into account local distortions and relaxation around vacancies. However, the static lattice displacement has been measured by neutron diffuse scattering in an L1₀-FePd by one of the present authors and has been found to be weak [7]. The use of symmetric interactions greatly reduces the number of simulation parameters without changing the order–disorder transition temperature [13]. Such a ‘toy model’ has been widely and successfully used to investigate the kinetics relaxation in binary systems [5, 13, 14]. The model is based on the atomic mechanism of order relaxation in dense phases [18]: vacancy–atom exchange between nearest-neighbour sites. The simulation starts with a perfect L1₀ ordered crystal in which one of the two sub-lattices (sub-lattice α) is occupied by A atoms and the other (sub-lattice β) by B atoms. To keep close to real systems and avoid any interaction effect between vacancies, only a single vacancy is introduced at random in the simulation box. The elementary Monte Carlo step is the following: one of the vacancy neighbours (A or B atom) is randomly chosen, the energy balance $\Delta\mathcal{H}$ of the atom–vacancy exchange before and after the jump is evaluated with the Ising Hamiltonian (equation (1)), considering the two nearest-neighbour shells of the initial and final atomic positions. The jump is performed if the Glauber probability [19]

$$P(\Delta\mathcal{H}) = \frac{1}{[1 + \exp(\Delta\mathcal{H}/k_B T)]} \quad (3)$$

is larger than a random number between 0 and 1. This corresponds to averaging the result over a large number of reversal jump attempts, the sum of the probabilities of the jump and its reversal being equal to 1.

The configuration of the system was analysed, at regular time intervals, by calculating two parameters: (i) an effective LRO parameter $\eta = 2(2N_A^\alpha - N_A)/(N_{\text{sites}} - 1)$, where N_A^α is the number of A atoms on the α sub-lattice and N_A is the total number of A atoms. (ii) APC = $\frac{N_{AB}^{\alpha\beta}}{N_B^\alpha}$, where $N_{AB}^{\alpha\beta}$ is the number of nearest-neighbour pairs of antisites and N_B^α is the number of α -antisites. The timescale is the number of jump attempts. One should keep in mind that the Monte Carlo time we refer to here is a ‘raw’ time. Its mapping to a physical timescale in seconds, in a system-specific study, requires knowledge of the physical properties, e.g. the vacancy concentration at different temperatures, diffusion coefficient etc. The relaxation of the LRO and the APC parameters towards their equilibrium values has been simulated in the z -variant, with (001)-type monoatomic layers of the L1₀ structure for different film thicknesses and different values of $k = V_2/V_1$. For each temperature, the evolution of η is followed until the system reaches equilibrium. We have chosen to stop when the simulation time is at least five times greater than the longer relaxation time of the system. The number of (001) layers has been varied from 8 up to 190 leading to more than 2000 simulations. Due to size effects, simulations of small film thicknesses suffered from poor statistics and very long relaxation times. All calculations have been performed on Pentium 4 processors using a Fortran 77 program.

3. Order–disorder transition

The equilibrium value of the LRO parameter η_{eq} versus temperature is plotted in figure 1 for different film thicknesses in the case $k = -0.2$. As expected, the order–disorder transition

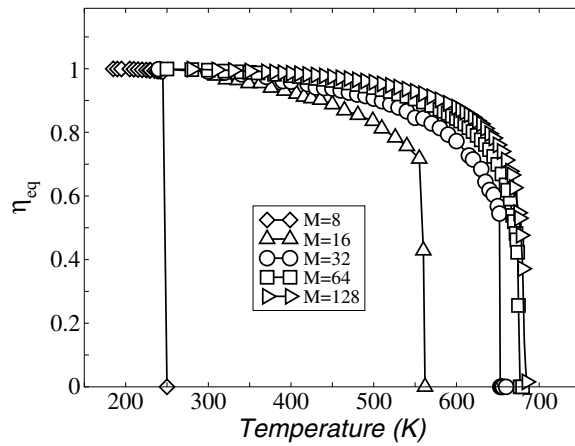


Figure 1. Equilibrium LRO versus temperature for different film thicknesses obtained for $k = -0.2$.

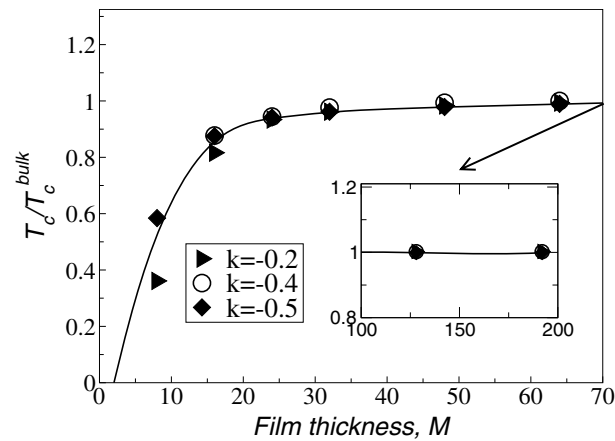


Figure 2. Reduced temperature versus film thickness for different values of k . T_c^{bulk} is the order-disorder transition temperature for $M \geq 128$. The line is a guide for the eye. The inset shows the asymptotic behaviour for higher film thicknesses.

temperature, T_c , decreases with decreasing film thicknesses as a result of the decrease in the relative number of atomic bonds caused by the symmetry breaking at the free surfaces. This behaviour is well seen in figure 2, in which the reduced critical temperature T_c/T_c^{bulk} is reported against the film thickness M for different values of k , T_c^{bulk} being defined as the transition temperature for film thicknesses greater than 128. The reduced transition temperature falls on a unique curve for all the pair interaction values, showing a plateau for $M \geq 64$, reflecting the bulk behaviour of the system. The extrapolation of the curve towards very thin films gives, in the limit $M = 1$, zero. Indeed, in this limit, the system reduces to one monoatomic plane containing only one kind of atom. The system then becomes unstable regardless of the sign of first and second nearest-neighbour pair interactions.

For small film thicknesses the order-disorder transition is found to be of first order type and the transition is clearly discontinuous. The calculated transition temperatures for $M \geq 64$ for different values of k agree quite well with previous Monte Carlo simulation of the LRO

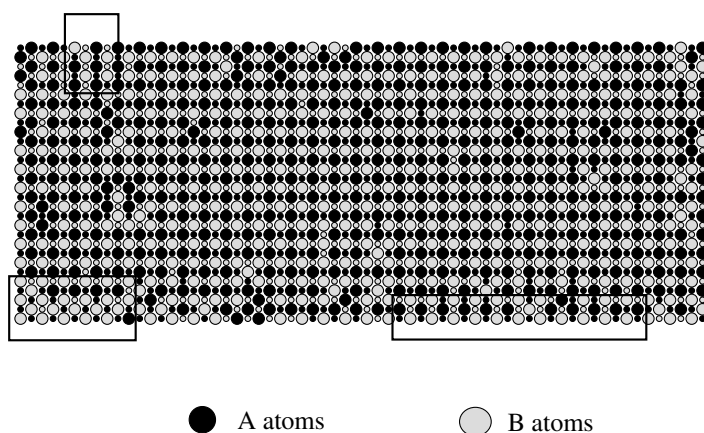


Figure 3. Snapshot of a (010) atomic plane (large circles) and its neighbouring plane (small circles) in an equilibrium state of an $L1_0$ thin film with 32 atomic layers at $T = 550$ K for $k = -0.2$. The boxes indicate nucleation of the x (upper and down left boxes) and y (lower right box) variants of the $L1_0$ structure.

relaxation in $L1_0$ bulk compounds [20]. For low and high film thicknesses as well, the transition temperature has been found, as expected, to be correlated to the ratio $k = V_2/V_1$.

Figure 3 shows a typical snapshot of two neighbouring (010) atomic planes obtained in the equilibrium state of a film containing 32 atomic layers at $T = 550$ K. It is clearly seen that the disordering takes place first at the free surfaces and then grows into the film. Nucleation of the x - and the y -variants of the $L1_0$ structure are also seen.

4. Two timescales ‘order–order’ relaxations

In good agreement with the predictions of the path probability method [21] and with many experimental and computational results in intermetallics [5, 14, 15, 22–25], the relaxations of the LRO have been found to be well fitted with the sum of two exponentials, yielding a long τ_1 and a short τ_s relaxation time:

$$\frac{\eta(t) - \eta_{\text{eq}}}{\eta(t=0) - \eta_{\text{eq}}} = C \exp\left(-\frac{t}{\tau_s}\right) + (1 - C) \exp\left(-\frac{t}{\tau_1}\right) \quad (4)$$

$0 \leq C \leq 1$. Figure 4 shows an example of the LRO relaxation towards the equilibrium value $\eta_{\text{eq}} = 0.72$ obtained for $M = 32$ with $k = -0.2$ and its fit using two exponentials. The coefficient values C of the fast relaxation process deduced from fits using equation (4) for different film thicknesses and different values of k are depicted in figure 5. Note that presenting the results as a function of the LRO is equivalent to presenting them as a function of temperature. In good agreement with previous Monte Carlo simulation of the kinetics relaxation in bulk $L1_0$ -FePd [15], the fast process is dominant for $M = 64$. Its contribution to the overall relaxation, however, decreases from $C \geq 0.9$ down to 0.78 for $M = 32$ ($k = -0.2$, $\eta_{\text{eq}} = 0.90$). For low enough thicknesses and high ordering states, the fast process smears out and the slow one becomes dominant ($C \leq 0.4$). A detailed study in the $L1_2$ phase has shown that the short relaxation time is related to the formation of the nearest-neighbour antisite pairs, whereas the longer one is related to the uncoupling of these antisite pairs [14]. The $L1_2$ phase of AB_3 compounds is also an fcc-based structure, but with a stoichiometric proportion $N_A/N_B = 1/3$. The A atoms occupy the cubic cell corners and the B atoms occupy the centre

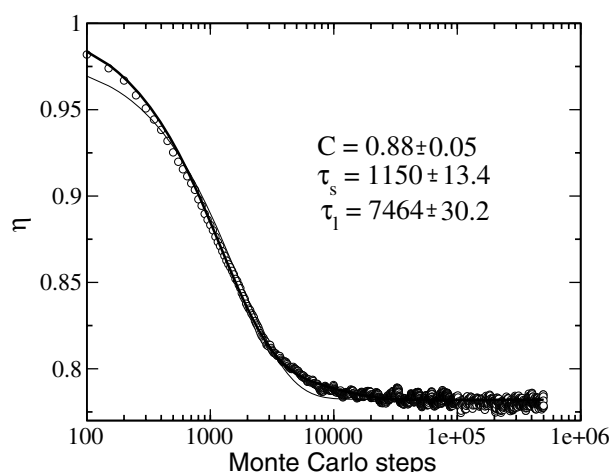


Figure 4. Semi-log plot of the isothermal relaxation of η obtained for $T = 950$ K and $k = -0.5$ for $M = 48$ (circles) and its simulation using the sum of two exponentials (thick line). For comparison, a fit using a single exponential is also shown (thin line).

of faces. The striking feature of figure 5 is that for low film thicknesses ($M = 16$) the same final degree of order ($\eta_{\text{eq}} = 0.90$) is reached through different processes, depending on the pair interaction energies. For $k = -0.2$ the fast process contributes a fraction of 35% to the overall relaxation whereas when $k = -0.5$ the fast process contributes more than 68%, stressing both geometrical and energetic effects on the feature of ‘order–order’ relaxations. To further investigate this point, we have calculated the relaxation of the APC parameter towards its equilibrium value for different film thicknesses with nearly the same final state of order ($\eta_{\text{eq}} = 0.90$ for $k = -0.2$ and $\eta_{\text{eq}} = 0.96$ for $k = -0.5$). The results are depicted in figure 6. For small film thicknesses, namely $M = 16$, where the contribution of the fast process is less than 40%, the early disordering stages are accompanied by a very fast increase of APC which reaches a maximum value before starting to decrease, while the effective LRO parameter decreases further. This behaviour is not seen in cases where the fast process is dominant, that is for film thicknesses $M = 32, 64$. The fast decrease of the LRO in the early stage of relaxation is due to the formation of nearest-neighbour pairs of antisites (increase of APC in figure 6). This process is very efficient in quickly decreasing the LRO. However, after a while it saturates, and a further decrease in the LRO (slow process) is due to the uncoupling of these nearest-neighbour antisite pairs which give rise to single antisite diffusion jumps (decrease of APC in figure 6). In both $L1_2$ and $L1_0$ structures antisite atoms may easily migrate within one sublattice without inducing any disorder. This process was shown to be responsible for the slow relaxation process in $L1_2$ -ordered compounds due to the uncoupling of the nearest-neighbour antisite pairs. Such events occur in the $L1_0$ structure within the basal planes and only four jump possibilities are offered, in comparison to eight in the $L1_2$ structure. As a result, such antisite diffusion jumps are definitely rare in $L1_0$ compounds in comparison to $L1_2$ compounds. This explains the very low contribution of the slow process in bulk $L1_0$ compounds. However, by reducing the z -axis dimension, the fraction of such jumps become equal to or even higher than that all possible jumps, giving rise to a dominant slow relaxation process, obtained in the case of $M = 16$ (figure 6).

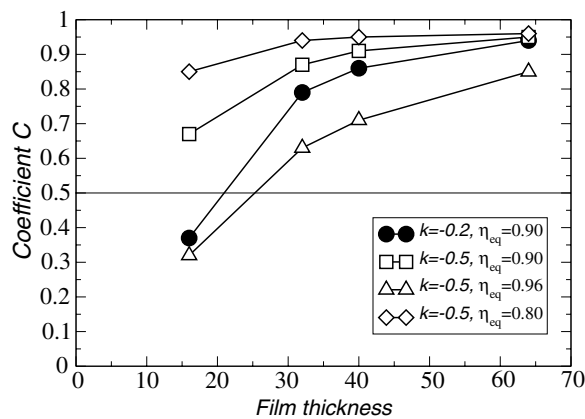


Figure 5. Variation of the coefficient C of the fast relaxation process versus film thickness for different values of k and different states of order. Note that presenting the results as a function of the LRO is equivalent to presenting the results as a function of temperature.

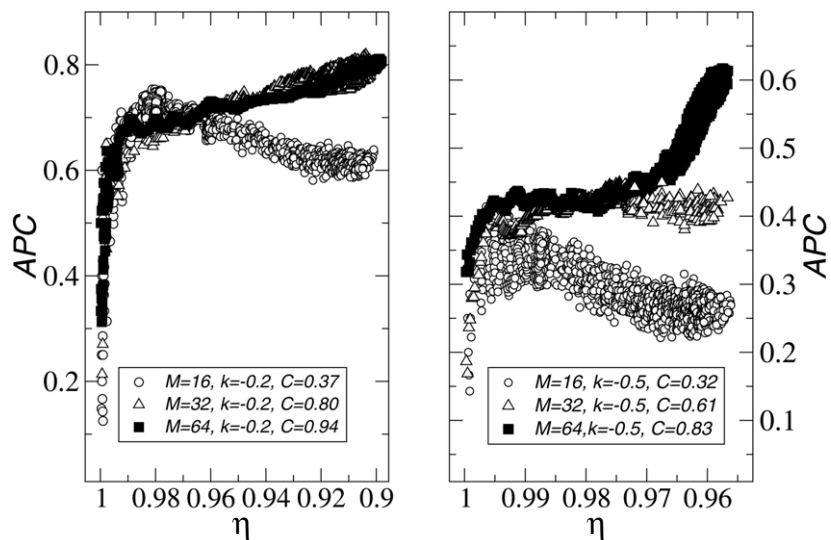


Figure 6. APC versus η during the relaxation of the systems with $M = 16, 32$ and 64 towards the equilibrium value $\eta_{eq} = 0.90$ for $k = -0.2$ (left) and $\eta_{eq} = 0.96$ for $k = -0.5$ (right).

5. Vacancy migration energy

The longer relaxation time, τ_1 , was found to follow an Arrhenius law yielding a vacancy migration energy E_M , which has been deduced from the linear regression of the Arrhenius plots for different film thicknesses M in the case $k = -0.2$ (figure 7). The increase in E_M for small film thicknesses can be explained by the fact that the thinner the film the smaller the degrees of freedom of the atomic motion. The film thickness effect is strong not only on the migration energy but also on the diffusion process itself. Depending on the film thickness, the final equilibrium state is reached by different routes (see figure 6) along which the vacancy encounters different atomic surroundings, leading to different migration energies.

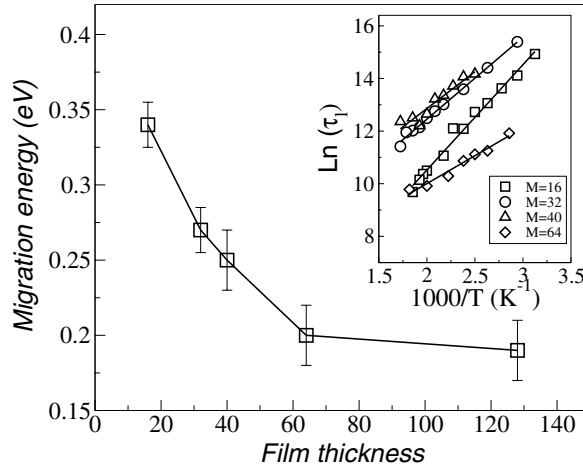


Figure 7. Variation of E_M with film thickness for $k = -0.2$. Inset: Arrhenius plots of the longer relaxation times.

If one extrapolates E_M towards very small film thicknesses, namely $M = 1$, we get a migration energy of 0.40 ± 0.05 eV. Kerrache *et al* [17] have obtained a linear variation of E_M with k for binary two-dimensional lattice. The linear extrapolation of their data to $k = -0.2$ leads to $E_M = 0.37$ eV, in good agreement with the present deduction. One should, however, keep in mind that $E_M = 0.40$ eV is the extrapolation from $M = 16$ towards very small thicknesses, thus the comparison is rather qualitative. Smaller film thicknesses are necessary for any further discussion; they were, however, extremely difficult to simulate within reasonable CPU time.

Different experimental methods have been used to determine activation energies in $L1_0$ FePt and CoPt thin films and multilayers. Grazing incidence synchrotron reflection (GIRNS) [26] has been used to measure the diffusion coefficient at different temperatures in FePt multilayers. Due to the geometry of the set-up used, only the activation energy along the c -axis could be measured. It has been found to be equal to 1.65 eV, which differs from extrapolation of high temperature tracer data [27]. Resistivity measurements showed that the activation energy drops from 2.7 eV for $T \geq 830$ K to 1.5 eV for $T \leq 800$ K [26]. The latter value agrees quite well with those deduced from the shift with temperature of the differential scanning calorimetry peak of the order–disorder transition with heating rate in FePt thin films (1.6 eV) [28]. The same analysis in CoPt thin films yields an activation energy of 2.8 eV. It is believed that the diversity of activation energies in FePt multilayers results from the variety of processes involved in the relaxations. Assuming that the activation energy, E_A , is the sum of E_M and the vacancy formation energy E_F , the simulated values of E_M agree qualitatively well with the experimental data. In our study, we keep a constant number of vacancies, therefore we do not have access to E_F . The vacancy formation energy E_F has been measured in pure Co, Pt [29] and Fe [30], and has been found equal to 1.38, 1.2 and 1.8 eV for Co, Pt and Fe, respectively. Considering the simulated $E_M = 0.40 \pm 0.05$ eV obtained for the smallest film thickness $M = 16$ for $k = -0.2$ in figure 7, added to an average value of E_F in the pure Co and Pt component, we get an activation energy in CoPt of 1.7 eV, which has to be compared to 2.8 eV measured in equiatomic CoPt thin films. A better agreement is obtained in the case of FePt. With the same approach we get $E_A = 1.9$ eV, which agrees well with the measured activation energy in FePt thin films given above. The better agreement observed for FePt in comparison to CoPt is not fortuitous. Paudyal *et al* have calculated the pair interaction energies

in L1₀-CoPt and FePt using first-principles calculations [31]. They give $V_1^{\text{FePt}} = 19.72$ meV, $V_2^{\text{FePt}} = -0.51$ meV for FePt and $V_1^{\text{CoPt}} = 27.33$ meV, $V_2^{\text{CoPt}} = -0.034$ meV for CoPt. The value of the first pair interaction of FePt used in our calculations is very close to the calculated value.

6. Conclusion

A Monte Carlo method was applied to investigate the relaxation of the LRO in dimensionally reduced L1₀ compounds. The order–disorder transition has been found to be first-order for small film thicknesses and, as expected, its temperature is strongly dependent on the pair interaction energies. A substantial increase in the migration energy has been obtained for small film thicknesses. By analysing the relaxation of the LRO and the antisite pair correlation parameters, we could stress that both geometrical and energetic effects play an important role in the interplay between the fast and the slow relaxation processes during ‘order–order’ relaxations. Despite the simplicity of our model, which does not take into account the substrate effect and assumes temperature independent interaction energies, we could qualitatively reproduce migration energies measured in L1₀ thin films and multilayers.

Acknowledgment

The authors would like to thank Dr V Pierron-Bohnes (CNRS/IPCMS Strasbourg, France) for carefully reading the first part of this manuscript and Professor J Schnack (Universität Osnabrück, Germany) for his corrections.

References

- [1] Tanaka K and Morioka K 2003 *Phil. Mag. A* **83** 1797
- [2] Leroux C, Cadeville M C, Pierron-Bohnes V, Inden G and Hinz F 1988 *J. Phys. F: Met. Phys.* **18** 2033
- [3] Morioka K 2002 *Master Thesis* Graduate School of Engineering, Kyoto University
- [4] Abes M, Ersen O, Elkaim E, Ulhaq-Bouillet C, Dinia A, Panissod P and Pierron-Bohnes V 2004 *Catal. Today* **89** 325
- [5] Kozubski R, Koslowski M, Pierron-Bohnes V and Pfeiler W 2004 *Z. Metallk.* **95** 10
- [6] Mehaddene T, Kentzinger E, Hennion B, Tanaka K, Numakura H, Marty A, Parasote V, Cadeville M C, Zemirli M and Pierron-Bohnes V 2004 *Phys. Rev. B* **69** 24304
- [7] Mehaddene T, Pierron-Bohnes V, Sanchez J M, Zemirli M and Caudron R 2004 *Eur. Phys. J. B* **41** 207–12
- [8] Mehaddene T 2005 *J. Phys.: Condens. Matter* **17** 485
- [9] Allalen M, Bouzar H and Mehaddene T 2005 *Eur. Phys. J. B* **45** 443
- [10] Messad L 2000 *Magister Thesis* Université Mouloud Mammeri, Tizi-Ouzou, Algeria
- [11] Koslowski M, Kozubski R, Pierron-Bohnes V and Pfeiler W 2005 *Comput. Mater. Sci.* **33** 287
- [12] Binder K 1976 *Phase Transitions and Critical Phenomena* vol 5b, ed C Domb and M S Green (London: Academic) p S 1
Binder K (ed) 1979 *Monte Carlo Methods in Statistical Physics* (Berlin: Springer) p S 1
- [13] Yaldram K, Pierron-Bohnes V, Cadeville M C and Khan M A 1995 *J. Mater. Res.* **10** 1–5
- [14] Oramus P, Kozubski R, Pierron-Bohnes V, Cadeville M C and Pfeiler W 2001 *Phys. Rev. B* **63** 174109
- [15] Mehaddene T, Adjaoud O, Kozubski R, Tanaka K, Numakura H, Sanchez J M, Issro Ch, Pfeiler W and Pierron-Bohnes V 2005 *Scr. Mater.* **53** 435
- [16] Ducastelle F and Gautier F 1976 *J. Phys. F: Met. Phys.* **6** 2039
- [17] Kerrache A, Bouzar H, Zemirli M, Pierron-Bohnes V, Cadeville M C and Khan M A 2000 *Comput. Mater. Sci.* **17** 324
Limoge Y and Bocquet J L (ed) 2001 *Proc. DIMAT 2000* (Uetikon-Zürich: Scitec) pp 403–9
- [18] Petry W, Heiming A, Herzig C and Trampenau J 1991 *Defect Diffus. Forum* **75** 211
- [19] Glauber R J 1963 *J. Math. Phys.* **4** 294
- [20] Kerrache A 2000 *Magister Thesis* Université Mouloud Mammeri, Tizi-Ouzou, Algeria

- [21] Sato H, Gschwend K and Kikuchi R 1991 *J. Phys.: Condens. Matter* **7** 357
- [22] Kozubski R and Pfeiler W 1996 *Acta. Mater.* **44** 1573
- [23] Lang H, Uzawa H, Mohri T and Pfeiler W 2001 *Intermetallics* **9** 9
- [24] Sattonay G and Dimitrov O 1999 *Acta. Mater.* **47** 2077
- [25] Kulovits A, Soffa W A, Püschl W and Pfeiler W 2003 *Mater. Res. Soc. Symp. Proc.* **BB5.37.1** 753
- [26] Kozubski R, Kozłowski M, Zapala K, Pierron-Bohnes V, Pfeiler W, Rennhofer M, Sepiol B and Vogl G 2005 *J. Phase Equilib. Diff.* **26** 482
- [27] Kushida A, Tanaka K and Numakura H 2003 *Mater. Trans.* **44** 59
- [28] Barmak K, Kim J, Shell S, Svdberg E B and Howard J K 2002 *Appl. Phys. Lett.* **80** 4268
- [29] Wollenberger H J 1983 *Physical Metallurgy* 3rd edn, ed R W Cahn and P Haasen (Amsterdam: Elsevier)
- [30] Schultz H 1991 *Atomic Defects in Metals (Landolt–Börnstein New Series Group III, vol 25)* ed H Ullmaier (Berlin: Springer)
- [31] Paudyal D, Saha-Dasgupta T and Mookerjee A 2004 *J. Phys.: Condens. Matter* **16** 7247